



Cite this: *CrystEngComm*, 2024, 26, 4156

Migration paths of the Na⁺-ion diffusion for minerals of the lovozerite group: crystallochemical and DFT modeling†

Natalia A. Kabanova  ^{ab}

For 11 minerals of the lovozerite group, theoretical investigations of Na⁺-ion migration were performed. The combination of GT, BVSE, and DFT-NEB approaches allows for studying the relationship between the crystallochemical energetic characteristics and ion-conductive properties of solid electrolytes. The constructed tilings made it possible to establish common types of cavities (tiles) for these structures. The location of sodium in large cavities suggests that these cavities can serve as new building blocks for modeling zeolite-like frameworks. GT analysis indicated that combeite, townendite, kapustinite and kazakovite have the widest Na⁺-migration paths among the 11 minerals. Using the BVSE approach, values of the migration barriers were obtained. For combeite, townendite, kapustinite and zolotarevite, the values of the migration barriers are in the range of 0.60–0.80 eV. DFT-NEB modeling results are in good agreement with the results from BVSE and GT analyses. It was found that minerals of this group have structures that are promising for the creation of new cation-conducting materials.

Received 30th May 2024,
Accepted 1st July 2024

DOI: 10.1039/d4ce00545g

rsc.li/crystengcomm

1. Introduction

Among the materials for metal-ion batteries, lithium minerals are in the highest demand. However, the importance of studies on sodium solid electrolytes has increased recently due to the low content of lithium materials in the earth's crust and the rapid growth in their price. Many prospective sodium-ion conductors have a crystal structure of one of the well-known mineral species: olivine,¹ apatite,² kaolinite,³ xenophyllite.⁴ Among silicates, the cation-conductive properties of the sugilite-type compound Fe₂Na₂K[Li₃Si₁₂O₃₀] have recently been described,⁵ and it has been established that their bulk ionic conductivity is 1.7×10^{-3} S cm⁻¹ at 943 K. For compounds with the lovozerite-type structures, ion conductance is also possible because of their sizeable channels and cavities. In a study,⁵ using the complex impedance method, the Sn- and Zr-containing compounds with lovozerite-type structures were investigated and it was established that the Na₃H₅ZrSi₆O₁₈ compound has an ionic conductivity of 5×10^{-4} S cm⁻¹ at 573 K. The ion-exchange properties of the minerals of the lovozerite group are also being actively studied; recently, a study of the inclusion of

potassium in the structure of combeite was carried out.⁵ Ten minerals of the lovozerite group are divided into three subgroups: the zirsinalite-lovozerite subgroup (zirsinalite, lovozerite, combeite, kapustinite, kazakovite, litvinskite, townendite and tisinalite), the koashvite subgroup (koashvite), and the imandrite subgroup (imandrite).⁶ In 2022, a new mineral was discovered in the Lovozero alkaline massif (Kola Peninsula, Russia) – zolotarevite, which was classified as a member of the zirsinalite-lovozerite subgroup.⁶ There are a large number of works devoted to the study of the crystal chemistry of minerals of this group.^{7–9} As indicated in a study,¹⁰ the first crystal chemical review of the structures of minerals of the lovozerite group was made by Chernitsova *et al.* (1975)¹¹ who proposed that all structures of minerals of the lovozerite group should be considered from the point of view of pseudocubic modules centered at the midpoint of the 6-MR ring. In another study,⁷ a local analysis of lovozerite mosaics was carried out and ten possible types of structures based on cubic S6R blocks were identified, four of which are realized in nature. This investigation of the cubic S6R blocks was also expanded.¹² However, the possibilities of sodium ion migration for minerals of this group of compounds have not previously been studied. A variety of different theoretical methods has been used for studying the ion conductors.^{13,14} The databases Bmaterials (<https://www.bmaterials.cn>), Materials Project (<https://materialsproject.org>), and BatteryMaterials (<https://batterymaterials.info>) were used to collect the measured and theoretical electrochemical and structure characteristics of the majority of solid electrolytes.

^a Laboratory of Nature-Inspired Technologies and Environmental Safety of the Arctic, Kola Science Centre, Russian Academy of Sciences, Fersmana str. 14, 184209 Apatity, Russia. E-mail: weterrster@gmail.com

^b Samara State Technical University, Molodogvardeyskaya Str. 244, Samara, Russia

† Electronic supplementary information (ESI) available. See DOI: <https://doi.org/10.1039/d4ce00545g>

The principles and fundamentals of multi-scale modeling are mostly collected in work,⁶ where both the theoretical foundations of computational materials science and part of the instructions for the experiment are presented. Among the works on the theoretical study of diffusion characteristics, several directions are most popular: crystal chemical analysis of empty space (geometrically-topological analysis (GT-analysis) by ToposPro,¹⁵ CAVD¹⁶ program); energy calculations of migration barriers using the bond valence method (bond valence site energy approach (BVSE approach), softBV¹⁷ program); DFT-NEB (nudged elastic band method within density functional theory) modeling of ion migration in the structure and assessment of the energy barrier (VASP¹⁸ program).

The combination of the GT, BVSE, and DFT-NEB approaches allows for studying the relationship between the crystallochemical, energetic characteristics and ion-conductive properties of solid electrolytes. Previously, we analyzed various groups of solid electrolytes using a combined approach.^{19–22} In the current work, the migration pathways of the sodium cation in the structures for the lovozerite group minerals were investigated.

2. Methods

2.1. Topological analysis of crystal structures

The topological analysis of the crystal structures is based on constructing the atomic net (framework net). The transformation of the 2-connected atoms to the edges of the net corresponded to the standard representation of the net.¹⁵ By means of calculating the net topological indices (coordination sequences, vertex symbols), the net topology can be unambiguously characterized and the topological type determined based on TTD-collections having about 800 000 entries (<https://topospro.com/databases/ttd/> or <https://topocryst.com>).²³ The theory of tiling²⁴ had successfully been applied to zeolites, which made it possible to describe (from a unified position) all zeolite blocks of which the frameworks are composed²⁵ and to predict new structures.²⁶ In addition, it has been established that tiles have a clear physical meaning and play a key role as elementary blocks during crystal growth.²⁷ The current TTT collection contains 428 natural tiles (included in the free ToposPro installation package). All zeolite tiles are collected in the Database of Zeolite Structures (<https://iza-structure.org>).

2.2. GT analysis of the Na⁺-migration paths

By means of the GT-analysis realized in the ToposPro program,¹⁵ many theoretical investigations of cation and anion solid electrolytes were performed.^{28–30} There are many theoretical investigations involving the screening of big data as an individual analysis for cation and anion solid electrolytes realized by the geometrical-topological analysis (GT-analysis) with the ToposPro program. The basis of the GT-method is a Voronoi partition,³¹ which is also named as the Voronoi tessellation.¹⁶ It divides the crystal space into

domains with the centers corresponding to the maximum of the electron density of the atoms. The vertices and edges of the Voronoi partition correspond to the maximal free crystal space. The analysis of the voids and edge parameters allows for estimating the available space for ion migration. To assess the possibility of placing an ion in a void or channel, a number of geometric criteria have been developed, such as void radius *Rsd*, channel radius $r_{\text{chan}(\text{min})}$, void shape G_3 , channel environment, *etc.*³² In this work, only the minimum channel radius parameter $r_{\text{chan}(\text{min})}$ was used. Previously, we were investigating the Na⁺-migration paths for cathode materials³³ and minerals.²¹ Upon comparing the calculated data of the migration maps with the experimental data on the conductivity of the cathode materials, it was determined that when the channel size $r_{\text{chan}(\text{min})}$ is less than 2.0 Å,³³ the sodium cation moves with difficulty; therefore, this value is crucial. We took the criterion of the minimal radius of channel $r_{\text{chan}(\text{min})} = 2.0$ Å to study the sodium-ion conductivity in the minerals of the lovozerite group.

2.3. BVSE approach and KMC modeling

The BVSE method is very important for the analysis of various solid electrolytes due to its accessibility and ease in obtaining the correct results of the energy of activation barriers.^{13,34} The method is based on the condition for maintaining a local balance of bond efforts.³⁵ Using the standard deviation of bond valence, the Global Instability Index (GII) can be calculated. It was determined that structures with $\text{GII} > 0.20$ are unstable.³⁶ The BVSE approach was implemented in the softBV program.³⁷ The isosurface visualization was obtained using VESTA.³⁸ The diffusion coefficients and the theoretical ion conductivity were computed using KMC simulations (Kinetic Monte-Carlo method³⁹) implemented in the softBV command line version.

2.4. DFT modeling

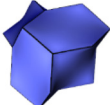
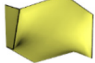
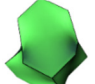
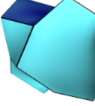

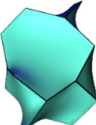
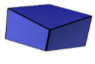

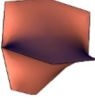
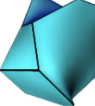
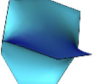
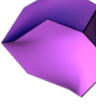



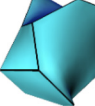
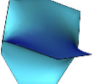

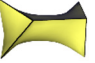

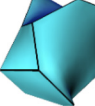
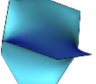


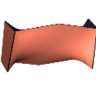
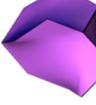

Quantum mechanical modeling within the DFT-NEB^{40,41} approach based on the generalized gradient approximation (GGA) with the Perdew–Burke–Ernzerhof (PBE) functional⁴² and projector augmented wave (PAW) pseudopotentials⁴³ was carried out by the Vienna *ab initio* simulation package VASP.¹⁸ The cutoff energy was fixed to 600 eV in all calculations. For the geometry optimization, the convergence thresholds for the total energy and force components were chosen as 10^{-5} eV and 10^{-4} eV Å⁻¹. Input files for NEB calculations were generated using the PATHFINDER script (<https://pathfinder.batterymaterials.info>). To visualize the NEB results, the ToposPro program¹⁵ was used.

3. Results and discussions

3.1. Topological features

Despite the fact that all 11 structures belong to the same group, the atomic net topologies of the crystal structures for

Table 1 Tilings for 5 types of atomic nets of the lovozerite group of minerals

Name of mineral	Topological type of the net	Tiles					Tiling
Combeite Litvinskite Lovozerite Townsendite Zolotarevite	sqc962 3,6-c net	 [6 ⁴ .8 ³] t-unkn ^a	 [4 ² .8 ²] t-kds	 [6 ³ .8 ³] t-unkn ^a	 [4 ² .8 ⁴] t-ste	 [4 ² .8 ⁴] t-ste	 [4 ² .7 ⁴ .8 ²] t-unkn3 ^a
Tisinalite	<i>New topology</i> 3,4,6-c net	 [4 ⁶] t-cub	 [4 ² .8 ²] t-kds	 [8 ³] t-jnt-1	 [4 ² .8 ⁴] t-unkn ^a	 [8 ³] t-jnt-1	 [4.5.7.8 ²] t-unkn2 ^a
Kapustinite Kazakovite Zirsinalite	<i>New topology</i> 3,4,6 ² -c net	 [4 ³] t-kzd	 [4 ⁶] t-cub	 [8 ³] t-jnt-1	 [4.5.7.8 ²] t-unkn ^a	 [8 ³] t-jnt-1	
Imandrite	<i>New topology</i> 3 ² ,4 ² ,6 ² -c net	 [4 ³] t-kzd	 [4 ² .6 ²] t-low	 [4 ² .5 ⁴] t-bru	 [4.5.7.8 ²] t-unkn ^a	 [8 ³] t-jnt-1	
Koashvite	<i>New topology</i> 3 ⁴ ,4 ⁴ ,6 ² -c	 [4 ³] t-kzd	 [4 ² .7 ²] t-unkn1 ^a	 [4 ² .8 ²] t-kds	 [4.5.7.8 ²] t-unkn2 ^a	 [4 ² .8 ⁴] t-ste	

^a Unknown topological type of tile, not included in the current version of the tile collection TTT.²⁵

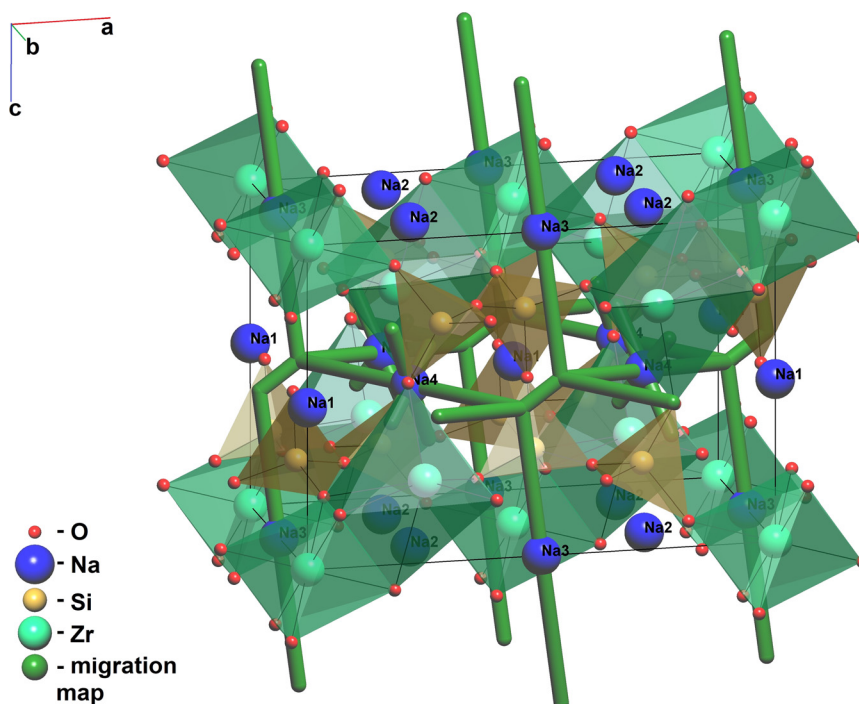
Table 2 Results of the GT analysis of the Na⁺-ion migration map for crystal structures of lovozerite group minerals

No.	Name	Formula (from IMA Database of Mineral Properties https://rruff.info/ima/)	Sp. gr.	Na ⁺ ion migration map for different values of minimal radius of channel, Å					ICSD code	Ref.
				1.90	1.95	2.00	2.05	2.10		
1	Combeite	Na _{4.5} Ca _{3.5} Si ₆ O _{17.5} (OH) _{0.5}	<i>R</i> 3̄ <i>m</i>	3D	3D	3D	3D	0D	62827	44
2	Litvinskite	Na ₃ ZrSi ₆ O ₁₃ (OH) ₅	<i>Cm</i>	3D	3D	0D	0D	0D	57042	45
3	Lovozerite	Na ₃ CaZrSi ₆ O ₁₅ (OH) ₃	<i>C</i> 2 ₁	3D	3D	1D[001]	0D	0D	30389	8
4	Townendite	Na ₈ ZrSi ₆ O ₁₈	<i>R</i> 3̄ <i>m</i>	3D	3D	3D	0D	0D	168092	46
5	Zolotarevite	Na ₅ Zr[Si ₆ O ₁₅ (OH) ₃]·3H ₂ O	<i>R</i> 3̄ <i>m</i>	3D	3D	0D	0D	0D	137779	6
6	Tisinalite	Na ₃ Mn ²⁺ TiSi ₆ O ₁₅ (OH) ₃	<i>P</i> 3̄	3D	3D	0D	0D	0D	250068	47
7	Kapustinite	Na ₆ ZrSi ₆ O ₁₆ (OH) ₂	<i>C</i> 2/ <i>m</i>	3D	3D	3D	0D	0D	250170	48
8	Kazakovite	Na ₆ Mn ²⁺ TiSi ₆ O ₁₈	<i>R</i> 3̄ <i>m</i>	3D	3D	3D	0D	0D	200602	48
9	Zirsinalite	Na ₆ CaZrSi ₆ O ₁₈	<i>R</i> 3̄ <i>c</i>	3D	3D	0D	0D	0D	200800	8
10	Imandrite	Na ₁₂ Ca ₃ Fe ³⁺ ₂ Si ₁₂ O ₃₆	<i>Pmnn</i>	3D	1D[001]	1D[001]	0D	0D	200805	49
11	Koashvite	Na ₆ CaTiSi ₆ O ₁₈	<i>Pmnb</i>	3D	2D(010)	1D[001]	0D	0D	86517	8

these compounds were of different types. The atomic net topologies were constructed with definitions involving the sodium cation located inside the cavities, *i.e.*, not included on net. The framework atoms (oxygen, silicon, calcium, zirconium, manganese, iron, titanium) correspond to the nodes of the atomic net. All calculated topological characteristics of tilings are given in Tables S1–S6,† and a visual representation of the tiling is given in Table 1. We see that the minerals, combeite, litvinskite, lovozerite, townendite, and zolotarevite have the same 3,6-connected net with topological type – **sqc962** (<https://epinet.anu.edu.au/sqc962>). There are two types of the nodes of this net: 3-connected nodes (Si or O) and 6-connected nodes (metal atoms). The tiling for

this net is isohedral, *i.e.*, contains one tile type – [6⁴.8³]. This type of tile was not found in the zeolite frameworks.

For the remaining six structures, the net belongs to a new topological type, characterized by the presence of different types of 3-, 4- or 6-connected nodes. For tisinalite, the tiling consists of three types of tiles; for kapustinite, kazakovite and zirsinalite, the tiling has 5 types of tiles; for imandrite - 7, and for koashvite - 8 types of tiles. It can be seen that almost all cavities can be named according to the zeolite classification and 6 new tile types discovered: [6⁴.8³], [6³.8³], [4.5.7.8²], [4².7²], [4².7⁴.8²]. Similar structural motifs of minerals are reflected in the same tiles for different minerals. The t-st-e tile was found for kapustinite, kazakovite,

**Fig. 1** Migration map of Na⁺ ions in the crystal structure of kapustinite.

zirsinalite, imandrite and koashvite. The t-kds tile is found in tisinialite, kapustinite, kazakovite, tisinialite and koashvite. Tiles t-kzd, t-lov, and t-cub are very small. They do not correspond to any cavity, but serve to fill the entire space.

3.2. GT-analysis

Silicates of the lovozerite group⁸ have sufficiently wide pores, in which water molecules or large cations are located. It was

Table 3 Disposition of Na atoms on the tiling and migration map for minerals of the lovozerite group

Mineral	Topological type	Atom position	Tile	Location on the tiling	Average distance Na–O, Å	Multiplcity of the position in the tile	Rsd, Å	Part of the migration map (GT analysis)
Combeite	sqc962	Na_{1,0,6}(Ca_{1,0,4})	[6 ⁴ ·8 ³]	Center of tile	2.40	1	1.49	3D map
		Na2	[6 ⁴ ·8 ³]	Center of 8-ring Si–Si–Si–Ca–Si–Si–Si–Ca	2.66	3	1.56	3D map
		Na _{3,0,6} (Ca _{2,0,4})	[6 ⁴ ·8 ³]	Center of 6-ring Si–Si–Ca–Si–Si–Ca	2.67	3	1.50	—
Litvinskite	sqc962	Na1	[6 ⁴ ·8 ³]	Center of 6-ring Si–Si–Zr–Si–Si–Zr	2.61	1	1.53	0D map
		Na _{2,0,78} (O _{1,0,22})	[6 ⁴ ·8 ³]	Center of 6-ring Si–Si–Zr–Si–Si–Zr	2.62	2	1.53	—
Lovozerite	sqc962	Na _{3,0,19} (Mn _{0,16})	[6 ⁴ ·8 ³]	Center of tile	2.43	1	1.49	0D map
		Na1	[6 ⁴ ·8 ³]	Center of 6-ring Si–Si–Zr–Si–Si–Zr	2.46	2	1.49	—
		Na_{2,0,5}(O_{11,0,5})	[6 ⁴ ·8 ³]	Center of 6-ring Si–Si–Zr–Si–Si–Zr	2.49	1	1.52	1D map
Townendite	sqc962	Na1	[6 ⁴ ·8 ³]	Center of 6-ring Si1–Si–Zr–Si–Si–Zr	2.42	3	1.50	—
		Na2	[6 ⁴ ·8 ³]	Center of 8-ring Si–Si–Si–Zr–Si–Si–Si–Zr	2.65	3	1.55	3D map
		Na_{3,0,66}(Ca_{0,08}Fe_{0,06}Mn_{0,08}Y_{0,07})	[6 ⁴ ·8 ³]	Center of tile	2.40	1	1.48	3D map
Zolotarevite	sqc962	Na _{1,0,95} (Mn _{0,05})	[6 ⁴ ·8 ³]	Center of 6-ring Si1–Si–Zr–Si–Si–Zr	2.66	3	1.50	—
		Na2	[6 ⁴ ·8 ³]	Center of tile	2.57	1	1.47	0D map
		Na _{3,0,11} (O _{4,0,89})	[6 ⁴ ·8 ³]	Center of 8-ring Si–Si–Si–Zr–Si–Si–Si–Zr	2.64	3	1.54	0D map
Tisinialite	New topology	Na1	[6 ³ ·8 ³]	Center of 6-ring Si–Si–Ti–Si–Si–Ti	2.33	3	1.46	0D map
		Na2	[6 ³ ·8 ³]	Center of 6-ring Si–Si–Ti–Si–Si–Ti	2.37	3	1.46	0D map
Kapustinite	New topology	Na1(Nd _{1,0,04})	t-ste [4 ² ·8 ⁴]	Center of tile	2.46	1	1.51	—
		Na2 (Nd _{2,0,03})	t-ste [4 ² ·8 ⁴]	Center of tile	2.45	1	1.51	—
		Na3	t-kds [4 ² ·8 ²]	Center of tile	2.62	1	1.54	3D map
		Na4	t-kds [4 ² ·8 ²]	Center of tile	2.67	1	1.56	3D map
Kazakovite	New topology	Na1	t-ste [4 ² ·8 ⁴]	Center of tile	2.37	1	1.48	—
		Na2	t-kds [4 ² ·8 ²]	Center of tile	2.61	1	1.53	3D map
Zirsinalite	New topology	Na1	t-kds [4 ² ·8 ²]	Center of tile	2.64	1	1.54	0D map
		Na2	t-ste [4 ² ·8 ⁴]	Center of tile	2.44	1	1.50	0D map
Imandrite	New topology	Na1	t-ste [4 ² ·8 ⁴]	Center of tile	2.38	1	1.48	—
		Na2	[4·5·7·8 ²]	Center of tile	2.61	1	1.52	1D map
		Na3	t-lov [4 ² ·6 ²]	Center of tile	2.67	1	1.56	1D map
Koashvite	New topology	Na1	t-ste [4 ² ·8 ⁴]	Center of tile	2.35	1	1.47	—
		Na2	[4 ² ·7 ⁴ ·8 ²]	Center of tile	2.40	1	1.48	—
		Na3	[4·5·7·8 ²]	Center of tile	2.46	1	1.49	—
		Na4	[4 ² ·7 ²]	Center of tile	2.59	1	1.55	1D map
		Na5	t-kds [4 ² ·8 ²]	Center of tile	2.50	1	1.51	—

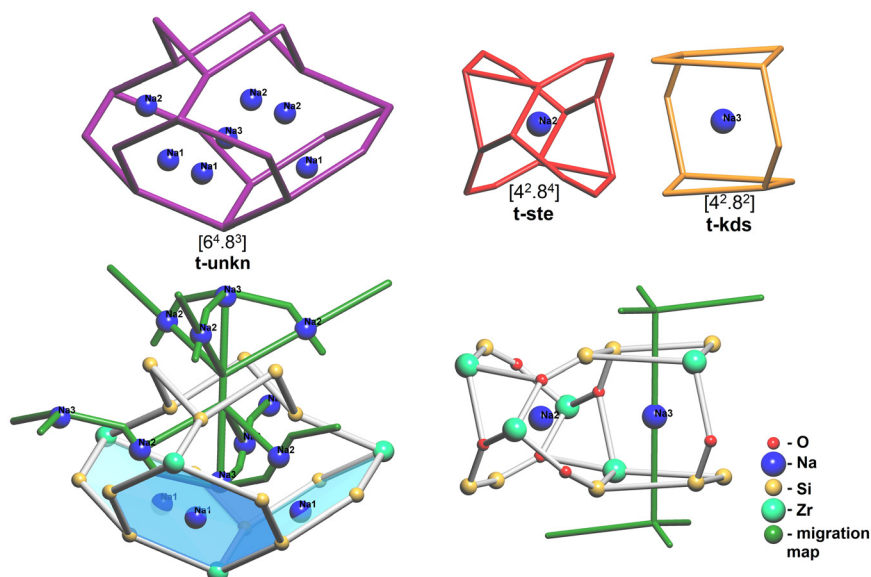


Fig. 2 Disposition of Na atoms inside the tiles for the townendite (left) and kapustinite (right) structures. Tiles $[6^4.8^3]$ conclude six Na atoms, t-ste and t-kds conclude the Na2 and Na3 positions in their center accordingly; fragments of the crystal structures corresponding to the tiles and migration maps (bottom). 6-rings Zr-Si-Si-Zr-Si-Si (tile $[6^4.8^3]$) are marked in blue to show the positions of the Na1 atoms in their center.

determined (Table 2) that litvinskite, tisinialite, zolotarevite and zirsinalite have a 0D migration map at $r_{\text{chan}(\text{min})} = 2.00 \text{ \AA}$ for the diffusion of Na^+ cations that corresponds to a difficult diffusion at room temperature.

In these structures, some channels have radius in the range of 1.90–1.95 Å that possibly will expand slightly at pressure or high temperature.⁵⁰ Imandrite, koashvite and lovozerite have a migration map in the form of chains along the [001] direction. The most branched and wide system of channels (3D migration map) for the Na^+ -ion diffusion in this group of minerals has the structures of combeite, kapustinite, kazakovite (Fig. 1), and townendite. The location

of sodium by positions in the minerals of the lovozerite group is described in detail in ref. 6.

To assess which types of sodium atoms will be more capable of diffusion, the localization of sodium atoms in the tiles and the Na–O distance were calculated and matched with the migration map (Table 3). For all 11 minerals (except lovozerite and tisinialite), one of the sodium atoms is located in the center of one of the big tiles. Lovozzerite, litvinskite, and tisinialite are cation-deficient structures,¹⁰ so they do not have wide migration paths for sodium ions through the center of the tiles. The sodium position on 6-rings in the structure of lovozerite

Table 4 Results of the BVSE calculations of the Na^+ -ion migration for the crystal structures of the minerals of the lovozerite group

No.	Name	Formula	Sp. gr.	Energy barriers Na^+ -ion migration ΔE_m , eV			GII	ICSD code
				1D	2D	3D		
1	Combeite	$\text{Na}_{5.27}\text{Ca}_3(\text{Si}_6\text{O}_{18})$	$R\bar{3}m$	0.61	0.61	0.61	0.19	62827
2	Litvinskite	$\text{Na}_3(\text{Zr}_{0.96}\text{Hf}_{0.02})\text{Si}_6\text{O}_{18}$	Cm	0.69	0.76	<5	0.41	57042
3	Lovozerite	$\text{Na}_{2.5}\text{Zr}_{0.5}(\text{Si}_6\text{O}_{15})(\text{OH})(\text{H}_2\text{O})_2$	$C2_1$	0.91	0.97	0.97	0.41	30389
4	Townendite	$\text{Na}_8\text{ZrSi}_6\text{O}_{18}$	$R\bar{3}m$	0.62	0.62	0.63	0.18	168092
5	Zolotarevite	$\text{Na}_{4.87}\text{Ca}_{0.05}\text{Mn}_{0.91}\text{Zr}_{0.88}\text{Si}_6\text{O}_{18}$	$R\bar{3}m$	0.66	0.66	0.78	0.28	137779
6	Tisinialite	$\text{Na}_{2.08}(\text{Mn}_{0.42}\text{Ca}_{0.13})(\text{Ti}_{0.47}\text{Zr}_{0.14}\text{Nb}_{0.13}\text{Fe}_{0.12})\text{Si}_6\text{O}_{12.6}(\text{OH})_{5.4}$	$P\bar{3}$	1.11	1.11	1.34	0.78	250068
7	Kapustinite	$\text{Na}_{5.31}\text{Mn}_{0.24}\text{Zr}_{0.91}\text{Nd}_{0.09}\text{Ti}_{0.1}\text{Si}_6\text{O}_{16}(\text{OH})_2$	$C2/m$	0.83	0.83	0.95	0.32	250170
8	Kazakovite	$\text{Na}_6\text{MnTi}(\text{SiO}_3)_6$	$R\bar{3}m$	0.93	0.93	0.93	0.21	200602
9	Zirsinalite	$\text{Na}_6\text{CaZrSi}_6\text{O}_{18}$	$R\bar{3}c$	0.93	0.93	0.93	0.18	200800
10	Imandrite	$\text{Na}_{12}\text{Ca}_3\text{Fe}_2(\text{Si}_6\text{O}_{18})_2$	$Pmnn$	0.91	1.03	1.03	0.21	200805
11	Koashvite	$\text{Na}_6(\text{Ca}_{0.9}\text{Mn}_{0.35})(\text{Fe}_{0.5}\text{Ti}_{0.5})(\text{Si}_6\text{O}_{18})$	$Pmnb$	1.06	1.06	1.07	0.19	86517

Energy barrier values are highlighted in colour: 0–0.90 eV < 0.90–1.20 eV < 1.20 eV .

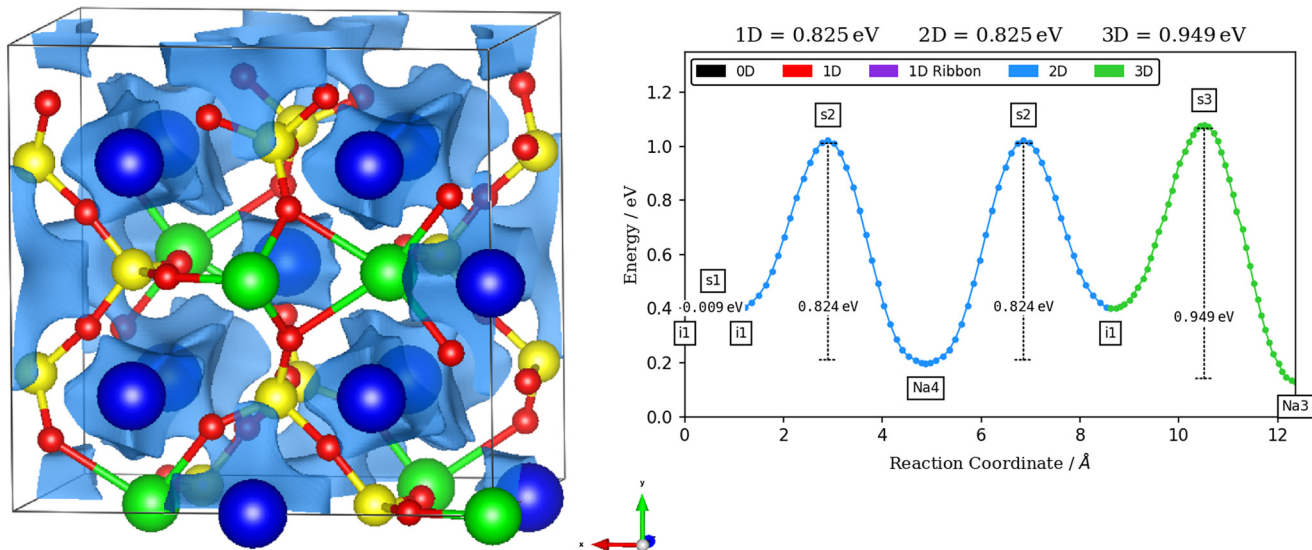


Fig. 3 Isosurface of the Na^+ ion diffusion for the kapustinite crystal structure and energy profile of the migration barriers obtained by the BVSE approach.

does not have geometric difficulties, and a one-dimensional migration map passes through it. This position is disordered and hence probabilistic. For cation-saturated minerals (townendite, combeite, kapustinite, kazakovite, zirsinalite, imandrite, koashvite, zolotarevite), the position of sodium in the center of the large cavity (tiles $[6^4 \cdot 8^3]$, $[6^3 \cdot 8^3]$, t-ste) is not involved in diffusion. For combeite and townendite, the migration map passes through the center of the $[6^4 \cdot 8^3]$ tile and 8-rings, and the 6-rings are not available for Na^+ diffusion (Fig. 2).

However, the central positions inside the tile are disordered. The t-ste cavity (kapustinite, kazakovite, zirsinalite, imandrite, koashvite) is quite large and it contains a sodium inside. However, it is not accessible for ion diffusion due to the small sizes of the windows (Fig. 2). As a result, the sodium atoms included on tiles t-kds, t-lov, $[4 \cdot 5 \cdot 7 \cdot 8^2]$, and $[4^2 \cdot 7^2]$ are arranged in a special way with each other to form channels available for Na^+ diffusion.

3.3. Energetic calculations

For all structures of minerals of the lovozerite group, the energy barriers were calculated using the BVSE approach in the softBV program (Table 3). To calculate the barriers, the initial structures were taken from the ICSD database, which contains the maximum available information on the composition of the unit cell. Accordingly, in structures with water molecules (lovozerite) or OH^- groups (lovozerite, tisinialite, kapustinite), the diffusion of sodium ions is hampered by the presence of these groups. The GII parameter for all structures indicates sufficient stability of the minerals, and the high value of $\text{GII} = 0.78$ for tisinialite is most likely associated with a large number of disordered positions (Table 4).

It has been established that from an energy point of view, sodium cations migrate along a 3D migration map in the structures of combeite, townendite, and zolotarevite, and

Table 5 Calculated results of the values of the ion diffusion coefficient and theoretical conductivity by KMC calculations for the kapustinite crystal structure

	Temperature, K				
	550	600	650	700	750
Mobility D , $\text{m}^2 \text{s}^{-1}$	1.28×10^{-18}	4.51×10^{-17}	1.44×10^{-7}	3.08×10^{-8}	5.74×10^{-7}
	1.79×10^{-18}	1.44×10^{-16}	2.23×10^{-8}	6.85×10^{-8}	1.06×10^{-6}
	2.06×10^{-17}	4.61×10^{-17}	3.08×10^{-8}	2.87×10^{-8}	2.02×10^{-7}
	2.89×10^{-18}	3.49×10^{-17}	8.66×10^{-8}	3.08×10^{-8}	5.94×10^{-7}
	1.82×10^{-18}	3.41×10^{-16}	4.24×10^{-9}	4.25×10^{-8}	6.36×10^{-8}
	5.68×10^{-18}	1.22×10^{-16}	5.76×10^{-8}	4.03×10^{-8}	4.99×10^{-7}
Ion conductivity σ , S cm^{-1}	6.39×10^{-18}	2.06×10^{-16}	6.04×10^{-7}	1.20×10^{-7}	2.09×10^{-6}
	8.74×10^{-18}	6.57×10^{-16}	9.40×10^{-8}	2.68×10^{-7}	3.85×10^{-6}
	1.02×10^{-16}	8.91×10^{-16}	1.30×10^{-7}	1.12×10^{-7}	7.37×10^{-7}
	1.44×10^{-17}	1.59×10^{-16}	3.64×10^{-7}	1.20×10^{-7}	2.17×10^{-6}
	9.04×10^{-18}	1.55×10^{-15}	1.78×10^{-8}	1.66×10^{-7}	2.32×10^{-7}
	2.78×10^{-17}	6.93×10^{-16}	2.74×10^{-7}	1.57×10^{-7}	1.82×10^{-6}

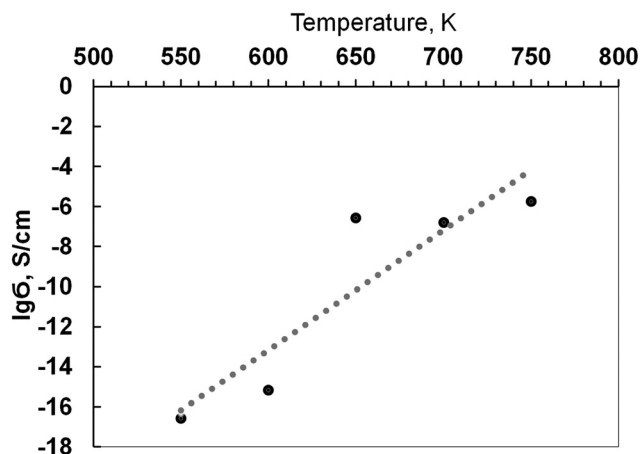


Fig. 4 Temperature dependences of the theoretically calculated ion conductivity for the kapustinite structure.

along a 2D migration map in the structures of litvinskite and kapustinite. For lovozerite, kazakovite, zirsinalite, koashvite and imandrite, the ion migration occurs in three directions, although it is restricted by the large energy barrier ($\Delta E_m > 0.90$ eV). For tisinalite, the barrier to the 3D migration is 1.34 Å, which suggests that geometric difficulties will not allow sodium to move in this direction even at elevated temperatures.

The isosurface showed a diffusion path of the Na^+ cation in the kapustinite crystal structure shown on Fig. 3. The value of the energy barriers indicates that the 2D migration map is preferable for this structure. For supercell $2 \times 2 \times 2$, the theoretical ionic conductivity and diffusion coefficient were computed using KMC simulations at 550 K, 600 K, 650 K, 700 K and 750 K. The KMC results were averaged over 5 different configurations (Table 5 and Fig. 4). The conductivity value is typical for sodium ion conductors,³³ and these values are expected among minerals.

Quantum mechanical modeling is one of the most time-consuming computational methods. The current work presents the results from the calculations of the energy barriers for kapustinite and zirsinalite (Table 6 and Fig. 5). It is convenient to determine the total number of migration paths using the developed online option service, <https://pathfinder.batterymaterials.info/>. For DFT calculations, the ideal structures (occupancy of all atoms equal 1) were made. For kapustinite and zirsinalite, a $1 \times 1 \times 2$ cell with the composition $\text{Na}_6\text{Mn}_2\text{ZrSi}_6\text{O}_{18}$ and a $1 \times 1 \times 1$ cell with the composition $\text{Na}_{12}\text{Ca}_4\text{Zr}_2\text{Si}_{12}\text{O}_{36}$ were modeled, respectively. The number of possible transitions between positions is 7 for kapustinite and 8 for zirsinalite, but only 2 and 4, respectively, are the shortest transitions for the sodium cation to jump from one position to another (Table 6).

The results from the calculations of the energy barriers using DFT modeling are in good agreement with the results from the BVSE and GT analyses. It can be seen both geometrically and energetically in the structure of zirsinalite that there are great difficulties for the diffusion of sodium ions, despite the fact that the structures have the same topology. The higher migration barrier for zirsinalite compared to kapustinite can be explained by the presence of a large calcium cation in its structure. This cation increases the repulsive interaction. The absence of a pronounced anisotropy of the ion conductivity can be characterized for all frameworks, and is confirmed by DFT calculations for kapustinite and zirsinalite.

4. Conclusion

A combination of theoretical approaches was used for the analysis of potential Na^+ -ion migration paths in the crystal structures of the lovozerite group. A comparison of the results of the topology analysis with the results of the

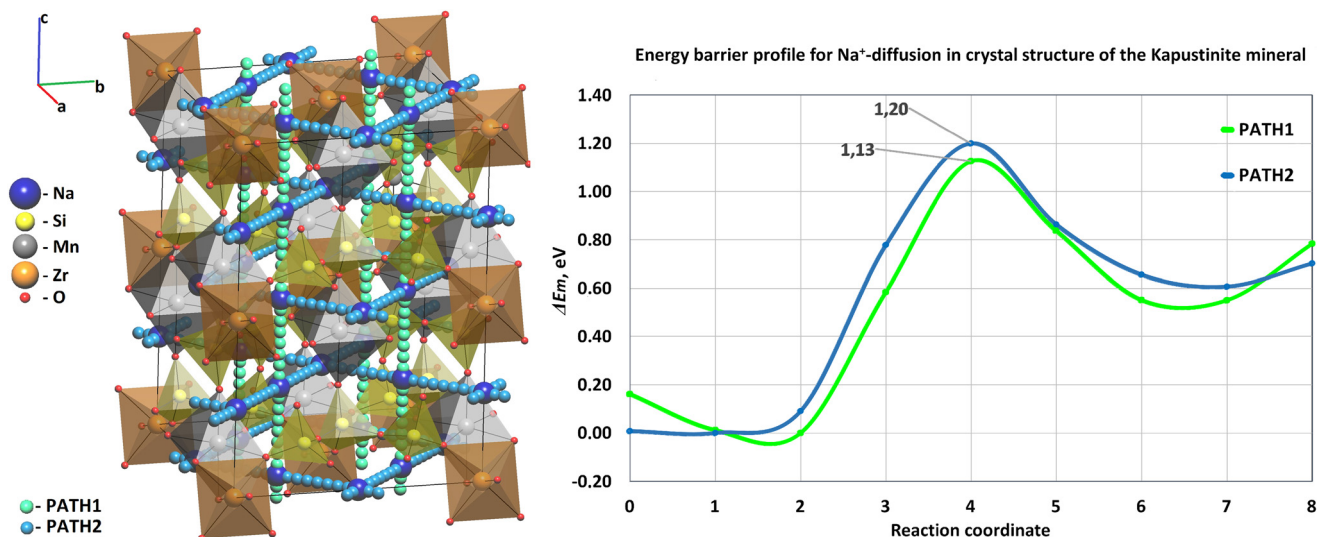


Fig. 5 Na^+ -ion diffusion map and energy barriers for the kapustinite structure obtained by DFT-NEB calculations.

Table 6 DFT-NEB calculation results for the determined Na⁺-ion migration barriers of the kapustinite and zirsinalite structures

Name	Super cell	Composition	Parameters of cell after optimization					Energy of energy barrier ΔE_m , eV			
			a, Å	b, Å	c, Å	V, Å ³	Energy of cell, eV	1D	2D	3D	ICSD
Kapustinite	1 × 1 × 2	Na ₆ Mn ₂ ZrSi ₆ O ₁₈	10.35	10.32	14.61	1559.3	-914.73	1.12	1.20	1.20	250170
Zirsinalite	1 × 1 × 1	Na ₁₂ Ca ₄ Zr ₂ Si ₁₂ O ₃₆	10.58	10.58	10.77	859.9	-451.65	1.31	1.31	1.31	200800

calculations of the migration paths shows that the sqc962 net corresponds to a prospective structure for the diffusion of sodium ions. The pathways of sodium movement in the structures were studied in detail, and the involvement of various sodium positions in diffusion was assessed. Tiling tessellation shows that the [6⁴-8³] and t-ste tiles likely participate in the formation of these structures. The location of sodium in large cavities suggests that these cavities can serve as new building blocks for modeling zeolite frameworks, or other microporous substances. These cavities are spacious, but the dense structure of the minerals makes it difficult for sodium to diffuse. Among the 11 minerals, the widest channels are found in combeite, townendite, kapustinite and kazakovite. The values of the migration barriers obtained using the BVSE approach (0.60–0.80 eV) for combeite, townendite, kapustinite and zolotarevite indicate the promise of these structures as ionic conductors. The inequality of energy barriers calculated by DFT modelling for kapustinite (1.2 eV) and zirsinalite (1.3 eV), which have similar structures, can be explained by the presence of different metal cations and different symmetries. In general, we can conclude that this class of structures is promising for ion diffusion and ion exchange. Thus, modifying the compositions will help to find promising materials for electrochemical batteries.

This research was performed in the framework of the state assignment 122022400093-9.

Data availability

Data are available upon request from the authors.

Conflicts of interest

There are no conflicts to declare.

Acknowledgements

I acknowledge V. A. Blatov and T. L. Panikorovskii for help with the work.

References

- 1 R. Tripathi, S. M. Wood, M. S. Islam and L. F. Nazar, Na-ion mobility in layered Na₂FePO₄F and olivine Na[Fe,Mn]PO₄, *Energy Environ. Sci.*, 2013, **6**(8), 2257–2264, DOI: [10.1039/c3ee40914g](https://doi.org/10.1039/c3ee40914g).
- 2 I. Es-saidi, J. Labrag, A. Laghzizil and J. M. Nunzi, Electrical and dielectric behaviors of thermally treated phosphate minerals, *Solid State Sci.*, 2021, **111**, 106440, DOI: [10.1016/j.solidstatesciences.2020.106440](https://doi.org/10.1016/j.solidstatesciences.2020.106440).
- 3 L. Zhou, J. Xu, M. Allix and X. Kuang, Development of Melilite-Type Oxide Ion Conductors, *Chem. Rec.*, 2020, **20**, 1117–1128, DOI: [10.1002/tcr.202000069](https://doi.org/10.1002/tcr.202000069).
- 4 S. N. Britvin, S. V. Krivovichev, E. V. Obolonskaya, N. S. Vlasenko, V. N. Bocharov and V. V. Bryukhanova, Xenophyllite, Na₄Fe₇(PO₄)₆, an Exotic Meteoritic Phosphate: New Mineral Description, Na-ions Mobility and Electrochemical Implications, *Minerals*, 2020, **10**(300), 1–13.
- 5 V. Kahlenberg, Concerning the incorporation of potassium in the crystal structure of combeite (Na₂Ca₂Si₃O₉), *Mineral. Petrol.*, 2023, **117**(2), 293–306, DOI: [10.1007/s00710-022-00801-2](https://doi.org/10.1007/s00710-022-00801-2).
- 6 J. A. Mikhailova, E. A. Selivanova, S. V. Krivovichev, Y. A. Pakhomovsky, N. V. Chukanov and V. N. Yakovenchuk, The new mineral zolotarevite, Na₅Zr[Si₆O₁₅(OH)₃]-2-3H₂O, the first highly hydrated lovozerite-group member from the Lovozero alkaline massif, Kola Peninsula, Russia, *Mineral. Mag.*, 2022, **86**(2), 263–271, DOI: [10.1180/mgm.2022.13](https://doi.org/10.1180/mgm.2022.13).
- 7 S. V. Krivovichev, Local approach and the theory of lovozerite structures, *Proc. Steklov Inst. Math.*, 2015, **288**(1), 105–116, DOI: [10.1134/S0081543815010083](https://doi.org/10.1134/S0081543815010083).
- 8 I. V. Pekov, S. V. Krivovichev, A. A. Zolotarev, V. N. Yakovenchuk, T. Armbruster and Y. A. Pakhomovsky, Crystal chemistry and nomenclature of the lovozerite group, *Eur. J. Mineral.*, 2009, **21**(5), 1061–1071, DOI: [10.1127/0935-1221/2009/0021-1957](https://doi.org/10.1127/0935-1221/2009/0021-1957).
- 9 Y. A. Malinovsky, H. Burzlaff and W. Rothammel, Structures of the lovozerite type – a quantitative investigation, *Acta Crystallogr., Sect. B: Struct. Sci.*, 1993, **49**(2), 158–164, DOI: [10.1107/S0108768192006529](https://doi.org/10.1107/S0108768192006529).
- 10 A. A. Zolotarev, Crystal chemistry of natural titanosilicates, *PhD thesis*, Saint Petersburg, 2019.
- 11 N. M. Chernitsova, Z. V. Pudovkina, A. A. Voronkov, Yu. L. Kaptin and Yu. A. Pyatenko, About the new cristellochemical family of lovozerite // Notes of the All-Union Mineralogist. Society, 1975, vol. 104(1), pp.18–27.
- 12 S. M. Aksenov and D. G. Stepenschikov, *Polymorphism of Lovozerite-type frameworks: features of the articulation of S6R blocks and principles of generation of new structures, presented at the XXVIII Russian Scientific Conference “Ural Mineralogical School – 2022”*.
- 13 B. He, *et al.*, High-throughput screening platform for solid electrolytes combining hierarchical ion-transport prediction algorithms, *Sci. Data*, 2020, **7**(1), 1–14, DOI: [10.1038/s41597-020-0474-y](https://doi.org/10.1038/s41597-020-0474-y).

- 14 D. Chen, J. Jie and M. Weng, *et al.*, High throughput identification of Li ion diffusion pathways in typical solid state electrolytes and electrode materials by BV-Ewald method, *J. Mater. Chem. A*, 2019, 7(3), 1300–1306, DOI: [10.1039/c8ta09345h](https://doi.org/10.1039/c8ta09345h).
- 15 V. A. Blatov, A. P. Shevchenko and D. M. Proserpio, Applied topological analysis of crystal structures with the program package topospro, *Cryst. Growth Des.*, 2014, 14(7), 3576–3586, DOI: [10.1021/cg500498k](https://doi.org/10.1021/cg500498k).
- 16 B. He, *et al.*, CAVD, towards better characterization of void space for ionic transport analysis, *Sci. Data*, 2020, 7(1), 1–13, DOI: [10.1038/s41597-020-0491-x](https://doi.org/10.1038/s41597-020-0491-x).
- 17 H. Chen, L. L. Wong and S. Adams, SoftBV - a software tool for screening the materials genome of inorganic fast ion conductors, *Acta Crystallogr., Sect. B: Struct. Sci., Cryst. Eng. Mater.*, 2019, 75(1), 18–33, DOI: [10.1107/S2052520618015718](https://doi.org/10.1107/S2052520618015718).
- 18 G. Kresse and J. Furthmüller, Efficient iterative schemes for *ab initio* total-energy calculations using a plane-wave basis set, *Phys. Rev. B: Condens. Matter Mater. Phys.*, 1996, 54(16), 11169–11186, DOI: [10.1103/PhysRevB.54.11169](https://doi.org/10.1103/PhysRevB.54.11169).
- 19 N. A. Anurova and V. A. Blatov, Analysis of ion-migration paths in inorganic frameworks by means of tilings and Voronoi-Dirichlet partition: A comparison, *Acta Crystallogr., Sect. B: Struct. Sci.*, 2009, 65(4), 426–434, DOI: [10.1107/S0108768109019880](https://doi.org/10.1107/S0108768109019880).
- 20 S. S. Fedotov, N. A. Kabanova, A. A. Kabanov, V. A. Blatov, N. R. Khasanova and E. V. Antipov, Crystallochemical tools in the search for cathode materials of rechargeable Na-ion batteries and analysis of their transport properties, *Solid State Ionics*, 2018, 314, 129–140, DOI: [10.1016/j.ssi.2017.11.008](https://doi.org/10.1016/j.ssi.2017.11.008).
- 21 N. A. Kabanova, *et al.*, The Na_{2–n}Hn[Zr(Si₂O₇)]·mH₂O Minerals and Related Compounds (n = 0–0.5; m = 0.1): Structure Refinement, Framework Topology, and Possible Na⁺-Ion Migration Paths, *Crystals*, 2020, 10(11), 1016, DOI: [10.3390/cryst10111016](https://doi.org/10.3390/cryst10111016).
- 22 N. A. Kabanova, Y. A. Morkhova, A. V. Antonyuk and E. I. Frolov, Prospective oxygen-ion conductors Ln_nX_bO_z: Geometry and energy calculations, *Solid State Ionics*, 2023, 391, 1116142, DOI: [10.2139/ssrn.4255822](https://doi.org/10.2139/ssrn.4255822).
- 23 A. P. Shevchenko, A. A. Shabalina, I. Y. Karpukhin and V. A. Blatov, Topological representations of crystal structures: generation, analysis and implementation in the TopCryst system, *Sci. Technol. Adv. Mater.: Methods*, 2022, 2(1), 250–265, DOI: [10.1080/27660400.2022.2088041](https://doi.org/10.1080/27660400.2022.2088041).
- 24 V. A. Blatov, O. Delgado-Friedrichs, M. O’Keeffe and D. M. Proserpio, Three-periodic nets and tilings: Natural tilings for nets, *Acta Crystallogr., Sect. A: Found. Crystallogr.*, 2007, 63(5), 418–425, DOI: [10.1107/S0108767307038287](https://doi.org/10.1107/S0108767307038287).
- 25 N. A. Anurova, V. A. Blatov, G. D. Ilyushin and D. M. Proserpio, Natural tilings for zeolite-type frameworks, *J. Phys. Chem. C*, 2010, 114(22), 10160–10170, DOI: [10.1021/jp1030027](https://doi.org/10.1021/jp1030027).
- 26 A. A. Golov, O. A. Blatova and V. A. Blatov, Perceiving Zeolite Self-Assembly: A Combined Top-Down and Bottom-Up Approach within the Tiling Model, *J. Phys. Chem. C*, 2020, 124(2), 1523–1528, DOI: [10.1021/acs.jpcc.9b10514](https://doi.org/10.1021/acs.jpcc.9b10514).
- 27 M. W. Anderson, *et al.*, Predicting crystal growth via a unified kinetic three-dimensional partition model, *Nature*, 2017, 544(7651), 456–459, DOI: [10.1038/nature21684](https://doi.org/10.1038/nature21684).
- 28 S. S. Fedotov, N. A. Kabanova, A. A. Kabanov, V. A. Blatov, N. R. Khasanova and E. V. Antipov, Crystallochemical tools in the search for cathode materials of rechargeable Na-ion batteries and analysis of their transport properties, *Solid State Ionics*, 2018, 314, 129–140, DOI: [10.1016/j.ssi.2017.11.008](https://doi.org/10.1016/j.ssi.2017.11.008).
- 29 R. A. Eremin, N. A. Kabanova, Y. A. Morkhova, A. A. Golov and V. A. Blatov, High-throughput search for potential potassium ion conductors: A combination of geometrical-topological and density functional theory approaches, *Solid State Ionics*, 2018, 326, 188–199, DOI: [10.1016/j.ssi.2018.10.009](https://doi.org/10.1016/j.ssi.2018.10.009).
- 30 V. I. Voronin, M. G. Surkova, G. S. Shekhtman, N. A. Anurova and V. A. Blatov, Conduction mechanism in the low-temperature phase of KAlO₂, *Inorg. Mater.*, 2010, 46(11), 1234–1241, DOI: [10.1134/S0020168510110130](https://doi.org/10.1134/S0020168510110130).
- 31 V. A. Blatov, G. D. Ilyushin, O. A. Blatova, N. A. Anurova, A. K. Ivanov-Schits and L. N. Dem’yanets, Analysis of migration paths in fast-ion conductors with Voronoi-Dirichlet partition, *Acta Crystallogr., Sect. B: Struct. Sci.*, 2006, 62(6), 1010–1018, DOI: [10.1107/S0108768106039425](https://doi.org/10.1107/S0108768106039425).
- 32 N. A. Anurova, V. A. Blatov, G. D. Ilyushin, O. A. Blatova, A. K. Ivanov-Schitz and L. N. Dem’yanets, Migration maps of Li⁺ cations in oxygen-containing compounds, *Solid State Ionics*, 2008, 179(39), 2248–2254, DOI: [10.1016/j.ssi.2008.08.001](https://doi.org/10.1016/j.ssi.2008.08.001).
- 33 S. S. Fedotov, N. A. Kabanova, A. A. Kabanov, V. A. Blatov, N. R. Khasanova and E. V. Antipov, Crystallochemical tools in the search for cathode materials of rechargeable Na-ion batteries and analysis of their transport properties, *Solid State Ionics*, 2018, 314, 129–140, DOI: [10.1016/j.ssi.2017.11.008](https://doi.org/10.1016/j.ssi.2017.11.008).
- 34 S. Adams and R. P. Rao, Transport pathways for mobile ions in disordered solids from the analysis of energy-scaled bond-valence mismatch landscapes, *Phys. Chem. Chem. Phys.*, 2009, 11(17), 3210–3216, DOI: [10.1039/B901753D](https://doi.org/10.1039/B901753D).
- 35 I. D. Brown, Recent developments in the methods and applications of the bond valence model, *Chem. Rev.*, 2009, 109(12), 6858–6919, DOI: [10.1021/cr900053k](https://doi.org/10.1021/cr900053k).
- 36 L. L. Wong, K. C. Phuah, R. Dai, H. Chen, W. S. Chew and S. Adams, Bond Valence Pathway Analyzer-An Automatic Rapid Screening Tool for Fast Ion Conductors within softBV, *Chem. Mater.*, 2021, 33(2), 625–641, DOI: [10.1021/acs.chemmater.0c03893](https://doi.org/10.1021/acs.chemmater.0c03893).
- 37 H. Chen, L. L. Wong and S. Adams, SoftBV – a software tool for screening the materials genome of inorganic fast ion conductors, *Acta Crystallogr., Sect. B: Struct. Sci., Cryst. Eng. Mater.*, 2019, 75(1), 18–33, DOI: [10.1107/S2052520618015718](https://doi.org/10.1107/S2052520618015718).
- 38 K. Momma and F. Izumi, VESTA 3 for three-dimensional visualization of crystal, volumetric and morphology data, *J. Appl. Crystallogr.*, 2011, 44(6), 1272–1276, DOI: [10.1107/S0021889811038970](https://doi.org/10.1107/S0021889811038970).

- 39 M. C. Simulations, M. Andersen, C. Panosetti and K. Reuter, A practical guide to surface kinetic Monte Carlo simulations, *Front. Chem.*, 2019, 7, 1–24, DOI: [10.3389/fchem.2019.00202](https://doi.org/10.3389/fchem.2019.00202).
- 40 P. Hohenberg and W. Kohn, Inhomogeneous Electron Gas, *Phys. Rev.*, 1964, **136**(3B), B864–B871, DOI: [10.1103/PhysRev.136.B864](https://doi.org/10.1103/PhysRev.136.B864).
- 41 G. Henkelman and H. Jónsson, Improved tangent estimate in the nudged elastic band method for finding minimum energy paths and saddle points, *J. Chem. Phys.*, 2000, **113**(22), 9978–9985, DOI: [10.1063/1.1323224](https://doi.org/10.1063/1.1323224).
- 42 J. P. Perdew, K. Burke and M. Ernzerhof, Generalized gradient approximation made simple, *Phys. Rev. Lett.*, 1996, **77**(18), 3865–3868, DOI: [10.1103/PhysRevLett.77.3865](https://doi.org/10.1103/PhysRevLett.77.3865).
- 43 P. E. Blöchl, Projector augmented-wave method, *Phys. Rev. B: Condens. Matter Mater. Phys.*, 1994, **50**(24), 17953–17979, DOI: [10.1103/PhysRevB.50.17953](https://doi.org/10.1103/PhysRevB.50.17953).
- 44 R. E. Fischer and E. Tillmanns, Revised data for combeite, *Acta Crystallogr., Sect. A: Found. Crystallogr.*, 1987, **43**, 1852–1854.
- 45 N. A. Yamnova, Y. K. Egorov-Tismenko, I. V. Pekov and I. A. Ekimenkova, Crystal structure of Litvinskite - a new natural representative of the lovozerite group, *Kristallografiya*, 2001, **46**(2), 230–234.
- 46 I. E. Grey, C. M. MacRae, W. G. Mummee and A. Pring, Townendite, Na₈ZrSi₆O₁₈, a new uranium-bearing lovozerite group mineral from the Ilímaussaq alkaline complex, Southern Greenland, *Am. Mineral.*, 2010, **95**(4), 646–650, DOI: [10.2138/am.2010.3293](https://doi.org/10.2138/am.2010.3293).
- 47 N. A. Yamnova, Y. K. Egorov-Tismenko, I. V. Pekov and L. V. Shegol'kova, Crystal structure of Tisinalite Na₂(Mn, Ca)_{1-x}(Ti,Zr,Nb,Fe³⁺)[Si₆O₈(O,OH)₁₀], *Acta Crystallogr., Sect. B: Struct. Sci.*, 2003, **48**(4), 551–556, DOI: [10.1107/s0567740872008374](https://doi.org/10.1107/s0567740872008374).
- 48 N. V. Zubkova, *et al.*, New Data on Mineralogy and Crystal Chemistry of the Lovozerite Group: Unusual Varieties of Kazakovite and Litvinskite, *Geol. Ore Deposits*, 2022, **64**(8), 657–669, DOI: [10.1134/S1075701522080128](https://doi.org/10.1134/S1075701522080128).
- 49 A. P. Homyakov, N. M. Chernicova, S. M. Sandomirskaya and G. Vasilieva, Imandrite - new minerals of lovozerite group, *Mineral. Zh.*, 1979, **1**, 89–93.
- 50 G. O. Kalashnikova, S. V. Krivovichev, V. N. Yakovenchuk, E. A. Selivanova, M. S. Avdontceva and G. Yu. Ivanyuk, *et al.*, The AM-4 Family of Layered Titanosilicates: Single-Crystal-to-Single-Crystal Transformation, Synthesis and Ionic Conductivity, *Materials*, 2024, **17**(1), 111–139, DOI: [10.3390/ma17010111](https://doi.org/10.3390/ma17010111).